RIEMANN SURFACES, TEICHMÜLLER SPACES, AND FENCHEL-NIELSON COORDINATES

EUGENIE CHA

Abstract

In this paper, we'll be proving the main theorem that T_S is homeomorphic to $\mathbb{R}_+^{3g-3} \times \mathbb{R}^{3g-3}$ where the mapping of this homeomorphism is the Fenchel-Nielson coordinates. To do this, we'll introduce some background. First, we'll introduce Riemann surfaces by looking at the square root function and the function that graphs a torus. Next, we'll discuss Teichmüller spaces by defining what markings on Riemann surfaces are. Finally, we'll discuss Fenchel-Nielson coordinates, which consists of topological pants decompositions and twisting angles.

1. Introduction

First, some historical background on these topics. In Bernhard Riemann's 1851 PhD dissertation, Riemann first combined works done by Niels Henrik Abel and Carl Gustav Jacobi to introduce the idea of Riemann surfaces. He further advanced his theory in his 1857 paper on the theory of abelian functions. Riemann's theories were studied in several different perspectives. Oswald Teichmüller wanted to more rigorously define Riemann's notion of moduli spaces, which yielded the Teichmüller space. This introduction of Teichmüller space developed into a field studying these spaces called Teichmüller theory, which consists of many notable contributions. One contribution we'll be discussing is by Jakob Nielson and Werner Fenchel. In their book [FN03], Nielson and Fenchel introduced the Fenchel-Nielson coordinates, which are coordinates for the Teichmüller space.

In this paper, we'll show that the Teichmüller space is homeomorphic to $\mathbb{R}_+^{3g-3} \times \mathbb{R}^{3g-3}$ and that the mapping of the space onto $\mathbb{R}_+^{3g-3} \times \mathbb{R}^{3g-3}$ is the Fenchel-Nielson coordinates. Here's a quick preview on some necessary background to prove this theorem.

Date: July 7, 2022.

If we say two objects are homeomorphic, this is equivalent to saying one object can be transformed into the other by molding it - as if it were clay. We define a "marking" on an object to be a unique path shaped like a loop on a surface. If we visualize the objects as clay, the markings on the objects can be thought of as drawing on the clay with a marker. For now, we can think of Teichmüller space as a collection of equivalent markings of objects. Points on this Teichmüller space can be defined by the Fenchel-Nielson coordinates, which record information about a surface.

To prove our main result, we'll first be providing all the necessary background. We'll introduce how Riemann surfaces are constructed and show some examples of them. Then, we'll define the Teichmüller space based off markings on Riemann surfaces. Finally, we'll introduce Fenchel-Nielson coordinates and use them to prove our main result.

2. Background

Definition 2.1. A **topological space** is a set with a topology, which allows for continuous deformation and continuity.

Definition 2.2. Two spaces are said to be **homeomorphic** if they can be deformed into each other by a continuous, invertible mapping.

For example, in figure 1, the leftmost shape is a donut and it can be molded - as if it was clay - into a coffee cup. This molding process does not include actions like tearing or ripping but merely pushing and pulling parts of the donut to form the coffee cup. We can say that the donut and coffee cup are homeomorphic. We denote homeomorphisms using the symbol $\approx$. It's often easier for mathematicians to show that two objects aren't homeomorphic. An example of objects that aren't homeomorphic is a sphere and a donut. These two are not homeomorphic because there is no way to mold the sphere such that it becomes a donut. This makes sense because no matter how much we pull or push the sphere, we won't be able to form the donut hole in a move that doesn't involve cutting or tearing.

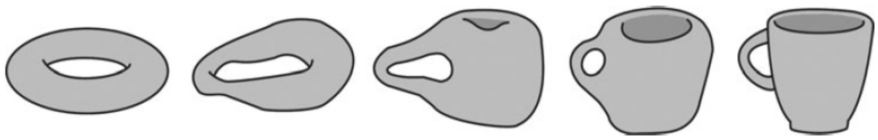

Figure 1. A diagram demonstrating that a donut and coffee cup are homeomorphic.

More important concepts in topology are the genus and boundary. The genus g counts the number of holes. For example, a donut has $g = 1$. The boundary n is the set of points not belonging to the interior of S and lying in the closure. A simpler way to think of this are the lines that delineate the shape.

We define the following terms that will be used throughout the paper.

Definition 2.3. A **holomorphic function** is a complex-valued function that's complex differentiable for each point in $\mathbb{C}^n$.

Definition 2.4. A **homeomorphism** is a continuous map with a continuous inverse.

Definition 2.5. A **diffeomorphism** is a differentiable map with a differentiable inverse

Definition 2.6. A **biholomorphism** is a holomorphism with a holomorphic inverse.

Definition 2.7. The **Euler characteristic** of a surface S is defined as $\chi(S) = v - e + f$ where v is the number of vertices, e is the number of edges, and f is the number of faces. For smooth surfaces, these values would be counted by counting the number of vertices, edges, and faces of the triangulation of this surface.

We won't go into the specifics of how we can triangulate a surface since we'll only use the Euler characteristic to derive basic theorems. In this paper, we'll use pre-calculated Euler characteristic values. From this definition, we have the theorem 2.8.

Theorem 2.8. *Given two orientable surfaces S_1 and S_2. S_1 is homeomorphic to S_2 if and only if $\chi(S_1) = \chi(S_2)$.*

Definition 2.9. The genus g can also be defined as $g = \dfrac{2 - \chi(S)}{2}$.

3. Riemann Surfaces

3.1. **The Square Root Function.** We start by considering the function $y = \sqrt{x}$ for all $x > 0$. Recall that the y values we obtain are the values we get when we solve the equation $x = y^2$. An example of an x value is 4. Intuitively, $y = 2$. However, y can also be -2 since y is being squared. In general, both $\sqrt{x}$ and $-\sqrt{x}$ will be solutions to y. Therefore, the graph of $y = \sqrt{x}$ will be the following:

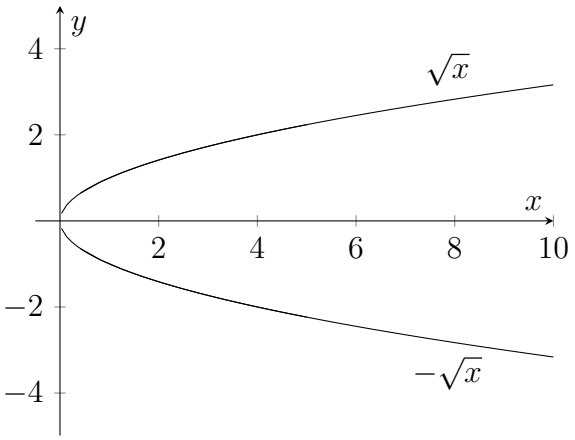

However, this is only for $x > 0$. Let's now look at the complex plane for all x such that $x < 0$. Similar to $x > 0$ case, we have the function $w = f(z) = z^{\frac{1}{2}}$, where z is a complex number and $\mathrm{Im}(z) \in \mathbb{R}$ and $\mathrm{Re}(z) \in \mathbb{R}$. Similarly, we're solving the equation $z = w^2$ for w. To determine whether this equation also has two solutions (like the $\sqrt{x}$ and $-\sqrt{x}$ we had earlier), we first express z in its polar form:

$$z = re^{i\theta}.$$

Recalling properties of polar form, we perform the square root computation:

$$w = \begin{cases} \sqrt{z} = \sqrt{r}e^{\frac{i\theta}{2}} \\ -\sqrt{z} = -\sqrt{r}e^{\frac{i\theta}{2}} \end{cases}$$

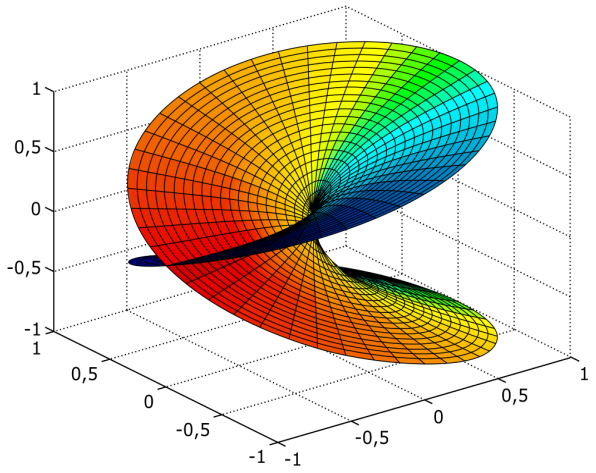

Figure 2. The full graph of $y = \sqrt{x}$ where the axes (x, y, z) are $(\mathrm{Re}(z), \mathrm{Im}(z), \mathrm{Re}(w))$. In this diagram, the y axis is the one extending to the left, and the x axis is extending to the right, while the z axis extends upwards.

If we want to graph our results similar to the real case, we run into a problem. Both the domain and range of the function are complex numbers. Recall that graphing complex numbers requires two dimensions: one real and one complex. This means graphing a complex input and output will require four dimensions. Because it's harder to work in four dimensions as we don't have a strong intuition for it, we project our four-dimensional graph down to three dimensions. We can assign our axes to be $(\mathrm{Re}(z), \mathrm{Im}(z), \mathrm{Re}(w))$. Now, the graph of $w = z^{\frac{1}{2}}$ is as shown in figure 2.

In this graph, we can identify the graph $y = \sqrt{x}$ for $x > 0$. In figure 3, we see the $y = \sqrt{x}$ graph in the red box. By tracing along the green portions of the graph, we have the parabolic-like shape that we saw for the real values.

This graph clearly shows the multi-valuedness of the square root function. This is called the **Riemann Surface** of $y = \sqrt{x}$.

Definition 3.1. A **Riemann surface** is a connected one-dimensional complex manifold.

The Riemann surface let's us visualize multi-valuedness. If we start on a point on the graph and circle around - specifically, a 2π revolution - we circle around to the same value but with an opposite sign. For example, if our starting point is on the top green region, after

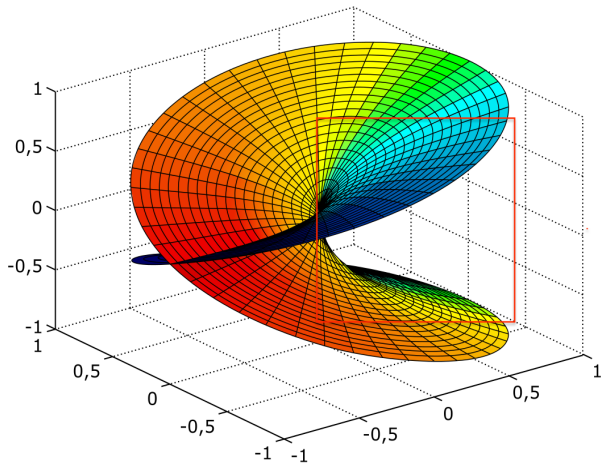

Figure 3. The full graph of $y = \sqrt{x}$ with the real parabola in the red boxed area

making a 2π revolution, we end up on the bottom green region. Mathematically speaking, we get the negative root.

This 2π revolution circling phenomenon can also be represented through **branch cuts**. Branch cuts are sometimes considered an alternate representation to Riemann surfaces.

Definition 3.2. A **branch cut** is a curve where a multi-valued function is discontinuous.

Alternatively, one can think of branch cuts as cuts that are made at **branch points**.

Definition 3.3. A **branch point** is a value at which a multi-valued function doesn't return to its initial value as a closed, continuous curve around the point is traced.

A way to make sense of these complicated definitions is our 2π revolution visualization. As noted previously, making a 2π revolution on the Riemann surfaces results in a root with the opposite sign. This is what definition 3.3 is referring to by "a function not returning to its initial value". If this is hard to believe through just the visual representation, we can also think of this mathematically. Recall that we can represent z in polar form:

$$z = re^{i\theta}.$$

When taking the square root, we have:

$$\sqrt{z} = \sqrt{r}e^{\frac{i\theta}{2}}.$$

Adding 2π:

$$\sqrt{r}e^{\frac{i(\theta+2\pi)}{2}} = \sqrt{r}e^{\frac{i\theta}{2}+\pi}.$$

This is clearly not the same value. In fact, it's the opposite in sign! Clearly, $f(x) = \sqrt{x}$ has a branch cut. More specifically, its branch cut is the negative real axis.

Proposition 3.4. *When a function has branch cuts, the Riemann surface can be defined such that when moving through the branch cut, we move from one sheet to the other. The same goes for moving from the other sheet back to the first.*

An important note to make that traveling past the branch cut results in a "jump" between two "plates". Looking at the Riemann surface of $f(x) = \sqrt{x}$ (figure 2), this makes sense. The branch cut of $f(x)$ is the intersection between the red section and the blue section (this is the negative real axis), and the two plates - one on top and the other below it - are connected by the branch cut. Let's say we start at a point on the yellow area on the top plate. As we travel along the surface in the counterclockwise direction (making a 2π revolution is counterclockwise), we pass the branch cut. Once we pass the branch cut, we end up on the bottom plate.

In addition to the square root function, some other well-known examples of Riemann surfaces are the $\log(x)$ and $\arcsin(x)$ functions. The Riemann surfaces of these functions are shown in figure 4.

3.2. **A More Interesting Example: the Torus.**

Let's take a look at a more interesting example.

Example. $w = \sqrt{(z^2-1)(z^2-k^2)}$ where $k \in \mathbb{C}$, $k \neq \pm 1$, and $(z, w) \in \mathbb{C}^2$ [Tel03]

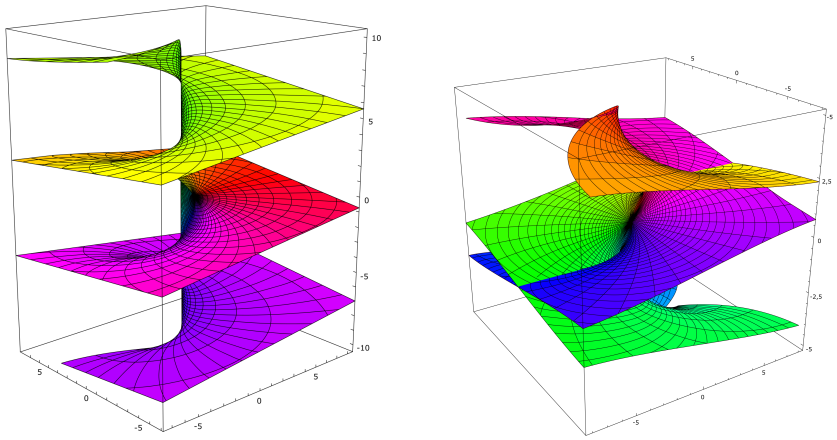

Figure 4. The Riemann surfaces for the functions $f(x) = \log(x)$ on the left and $f(x) = \arcsin(x)$ on the right.

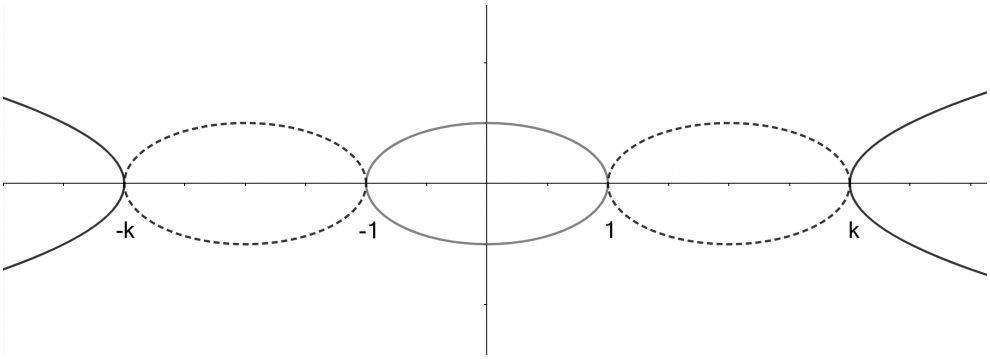

Figure 5. Number line showing where w is defined on the real plane. The dotted lines indicate imaginary-valued regions.

We take a similar approach by solving for w in

$$w^2 = (z^2 - 1)(z^2 - k^2).$$

The values for which w is defined in the real plane is $z \in (-\infty, -k] \cup [-1, 1] \cup [k, \infty)$, which can be visualized on a number line, where the dotted lines indicate imaginary values as shown in figure 5.

Near the points ± 1 and $\pm k$ the function behaves like a square root function. The important thing to note here is that there is no single value at these points. Recall in our earlier example of $f(x) = \sqrt{x}$, making a 2π revolution around the graph of the function - and therefore, the

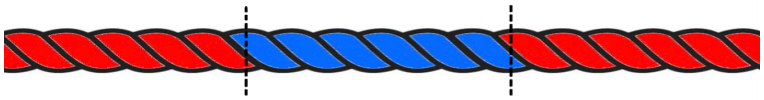

Figure 6. A rope with three segments; two red segments separated by a blue segment.

Figure 7. Representation of cutting out $(-k, -1)$ and $(1, k)$ and multi-valuedness of real values.

function itself - resulted in a root with the opposite sign. This implies that for any w if we follow continuously round ± 1 or $\pm k$ we'll end up with the opposite-signed root.

To define this continuous path, we need to make some "cuts" in our real plane. An easier way to visualize this is with a piece of string as shown in figure 6.

Let's define a "continuous" segment in this rope as a segment that has uniform color across the segment. We can think of the blue segment of rope as imaginary values while the red segments are real values. The imaginary values and real values aren't the same "color", which makes our "rope" not continuous. Therefore, we need to make cuts as shown in the figure.

To resolve this problem, we can remove the line segments $(1, k)$ and $(-k, -1)$. Additionally, on the complement of these segments, inputs have two outputs (think of the multi-valuedness of the square root function), so our graph must split into two different plates as shown in figure 7.

Notice that the function also takes on two values over the cut intervals due to the multi-valuedness on the imaginary-valued intervals as well. Also note that if we start on one plate and travel through the cut, we'll end up on the other plate. This follows from proposition 3.4. Therefore, if we start on one sheet and travel through the cut, we'll end up exiting on the other sheet. Thus, we have a path depicted as shown by the arrows in figure 8.

Figure 8. Representation of moving through the cuts across the sheets

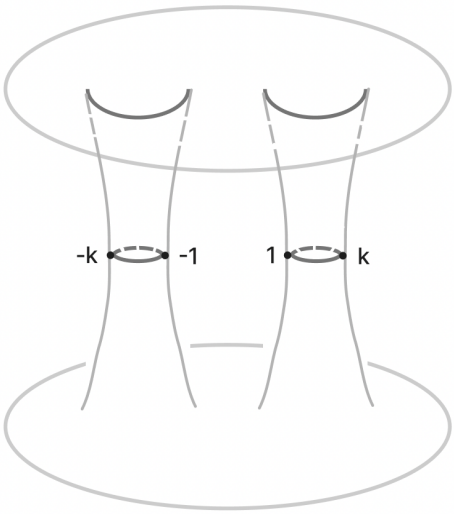

Figure 9. Representation of flipping a sheet and pulling out tubes

With the plates positioned as depicted, it would be impossible to create a model in $\mathbb{R}^3$ (the third dimension). In order to resolve this issue, we can flip one of the sheets about the real axis. In other words, multiply all the points on that sheet by $i^2 = -1$. Not only does this resolve our issue of modeling this in $\mathbb{R}^3$, but we also get a plate with opposite values, thereby resulting in a good representation of the function's multi-valuedness. Now that our cuts are aligned, we can pull out linking tubes as shown in figure 9.

There's another way to look at this surface. If we pull these tubes out until the infinitely large plates aren't plates, we end up with a donut-shaped object called the torus. The torus in this example, however, is slightly abnormal. Because we're pulling the tubes infinitely long, we'll end up with a torus as shown in figure 10.

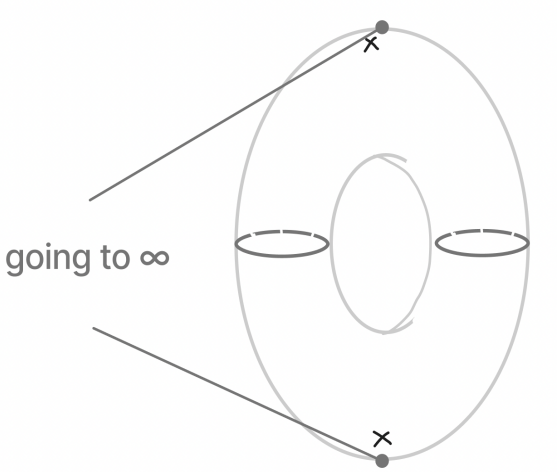

Figure 10. Another way to visualize figure 9

4. Teichmüller Spaces

Teichmüller spaces can be defined in serveral different ways. We'll be taking a look at the definition that uses marked Riemann surfaces. But first, some notation regarding Riemann surfaces. From now on, we'll be defining Riemann surfaces off of their genus g and their boundary component n. For more detailed definitions and explanations of these, refer to section 2.

4.1. **Marked Riemann Surfaces.**

Definition 4.1. The **fundamental group** is the group of equivalence classes under homotopy of the loops connected in the space. We can denote the fundamental group as $\pi_1(X, x_0)$ for a topological space X with base point x_0.

Intuitively speaking, the fundamental group records information about the number of loops that can be made on a surface from a **base point** x_0, where x_0 is a point on X.

The fundamental group is independent of the base point x_0. For a Riemann surface with genus g, the fundamental group consists of $2g$ elements. These elements make up a **marking** on a Riemann surface. We denote a marking on a surface of genus g as Σ_g.

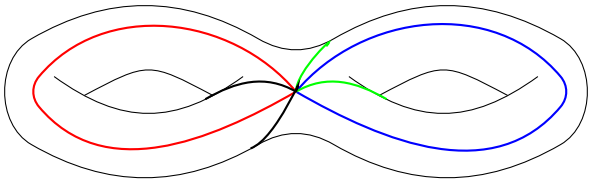

Figure 11. Torus of genus 2 with 4 markings.

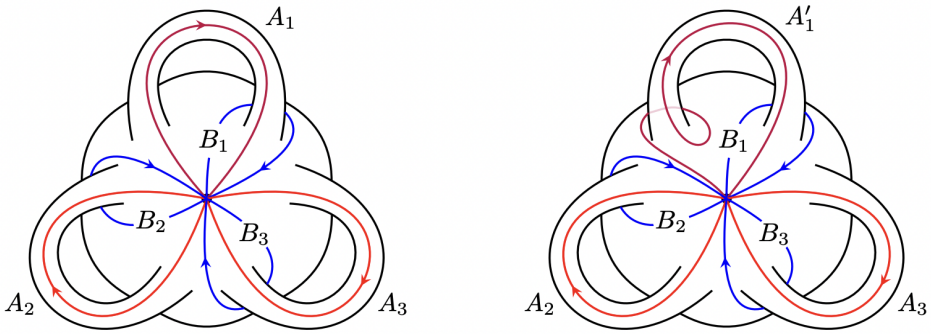

Figure 12. The collection of paths associated with markings $\Sigma_g = \{|A_1|, |A_2|, |A_3|, |B_1|, |B_2|, |B_3|\}$ (left) and $\Sigma_g = \{|A_1'|, |A_2|, |A_3|, |B_1|, |B_2|, |B_3|\}$ (right) on surfaces of genus 3. [Bro18]

Definition 4.2. For a Riemann surface R of genus g, a **marking** on R is defined as $\Sigma_g = \{|A_j|, |B_j| \,|\, j = 1, 2, ..., g\}$ of $\pi_1(R, p)$. We denote a **marked Riemann surface** R with marking Σ_g as (R, Σ_g).

Examples of markings can be seen in figures 11 and 12.

A question one might ask at this point is: can't there technically be infinite markings on a surface? We define two markings that originate from the same base point to be equivalent if they are homeomorphic to each other. In other words, one of the markings can be deformed into the other. For example, consider the markings on the genus 2 topological object shown in figure 13. The blue and red loops are considered equivalent because they are homeomorphic.

In addition to equivalent markings, we can define what it means for two marked Riemann surfaces to be equivalent.

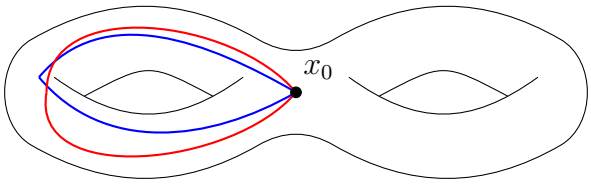

Figure 13. Genus 2 torus with two equivalent loops; one blue and one red

Definition 4.3. An **isometry** is a bijective map between two metric spaces that preserves distance.

Examples of isometries include translations, rotations, and reflections.

Definition 4.4. An **isotopy** is a homotopy from embedding one manifold X onto another Y such that it is an embedding.

Recall that a homotopy is a continuous family of homeomorphisms. For our purposes, we can treat an isotopy as a continuous function that is able to smoothly transform one manifold X onto another Y.

Definition 4.5. Two marked Riemann Surfaces (R, Σ_{g_1}) and (S, Σ_{g_2}) are considered **marking equivalent** if there exists an isometry $m : R \to S$ such that Σ_{g_2} and $m \circ \Sigma_{g_1}$ are isotopic.

Let's walk through this definition to make more sense of it. By our definition of an isometry (definition 4.3), R can be transformed to S such that distance is preserved. Furthermore, by our definition of isotopy (definition 4.4), there should exist a smooth transition from the marking Σ_{g_2} to $m \circ \Sigma_{g_1}$. We can now make sense of definition 4.5. Visually, it's saying that if we can make a continuous transformation (i.e: no cutting) from R to S such that we can smoothly transform Σ_{g_2} to Σ_{g_1}. In other words, if there is a function m that transforms R to S and this function also smoothly transforms the markings on R to the markings on S, then these surfaces are marking equivalent. This definition intuitively makes sense because as mentioned earlier, we defined equivalent markings as those that can be "deformed" into each other.

4.2. **The Teichmüller Space.**

Definition 4.6. We define the **Teichmüller space** of a Riemann surface S of genus $g \geq 2$ and boundary component n as

$$T_{g,n} = \{(S, \Sigma_g)\}/\sim$$

where Σ_g is the marking on S.

In other words, the Teichmüller space is the set of all marking equivalence classes for genus g and boundary component n. $T_{g,n}$ is different to the regular moduli space - the surface. Essentially, it's the moduli space but with markings. The reason we use markings - and therefore, Teichmüller space - is because it results in a much simpler space, which makes them easier to work with. Furthermore, for more complicated moduli with higher genuses, the moduli space becomes too complicated and eventually impossible to understand while the Teichmüller space is understandable. A natural question that arises from defining Teichmüller spaces is how we define points on it. This is the center of Fenchel and Nielson's work on Fenchel-Nielson coordinates.

5. Fenchel-Nielson Coordinates

Definition 5.1. A **pair of topological pants** is a genus zero surface with three boundaries.

An example of a pair of pants is shown in figure 14. One thing to note is that these pants can look slightly different. However, as long as it is homeomorphic to the pants shown in figure 14, it is considered a pair of pants. In addition to the genus and boundary requirements, there's another property of pants that we can note: **seams**.

Definition 5.2. Given a pair of pants with geodesic boundaries there exists three geodesic arcs that join the cuffs perpendicular to their endpoints. These arcs collectively are called the **seams** of the pants.

If we cut the pants along the seams, we end up with two hyperbolic hexagons with right angles. A representation of this can be seen in figure 15.

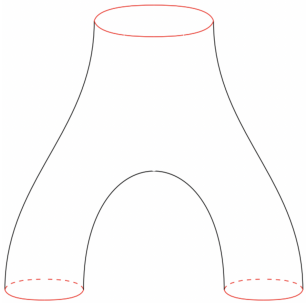

Figure 14. Topological pair of pants

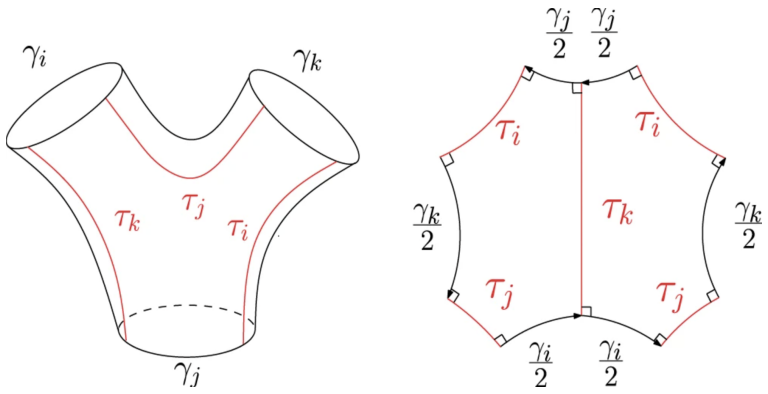

Figure 15. Representation of ending up with two hexagons when cutting along the seams of a pair of pants [SZS+16]

All pairs of pants have seams, and we can essentially define a pair of pants by defining its seams.

Proposition 5.3. *For $l_1, l_2, l_3 \in \mathbb{R}_+$, there exists a unique hyperbolic right-angled hexagon with alternating edge lengths (l_1, l_2, l_3).*

The most important takeaway from this proposition is that we can define a hyperbolic right-angled hexagon by three real, positive side lengths.

Proposition 5.4. *Given a surface S with genus g and pants decomposition P, the surface can be decomposed in $2g-2$ pairs of pants.*

Proof. Some things to note before starting the proof is that a pair of pants has an Euler characteristic of -1 and circles have an Euler characteristic of 0. Since the edges of the pairs of pants that are glued to each other are circles, they don't contribute to the Euler

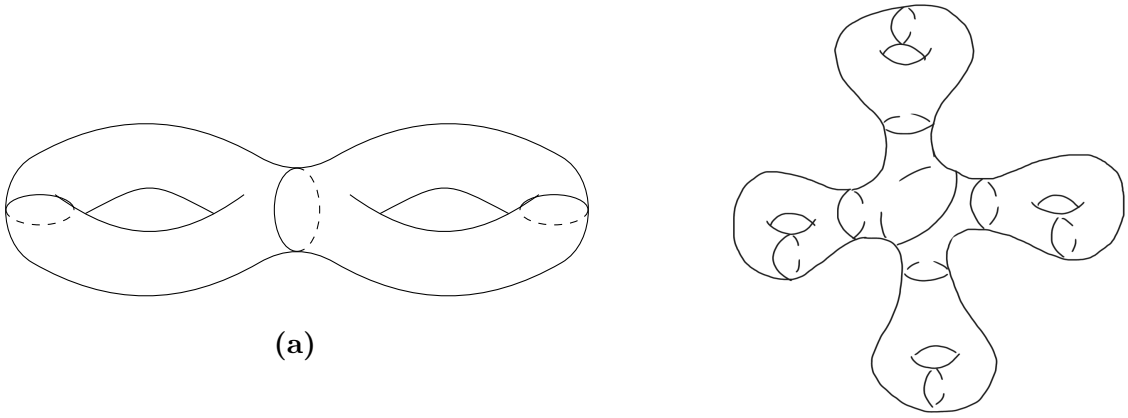

(a) **(b)**

Figure 16. Pants decomposition of a genus 2 surface (a) and a genus 4 surface (b)

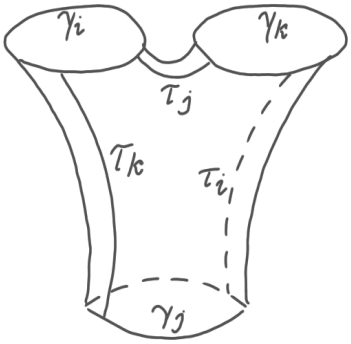

Figure 17. Pair of pants labeled with geodesic arcs τ_i, τ_j, and τ_k and boundaries γ_i, γ_j, and γ_k. [JZDG09]

characteristic. Therefore, each pair of pants in the decomposition will contribute exactly -1 to the Euler characteristic. So the number of pants $n = -\chi(S)$. Recall from definition 2.9 that $g = \dfrac{2-\chi(s)}{2}$. Substituting yields $n = 2g - 2$. ■

Some examples of decompositions of surfaces are shown in figure 16.

A **geodesic** is a length minimizing curve. Assume all of the boundaries in figure 17 $\{\gamma_1, \gamma_2, ..., \gamma_{3g-3}\}$ are geodesics. For each pair of pants, define the lengths $\{\tau_1, \tau_2, ...\tau_{3g-3}\}$ as the shortest paths between these boundaries. These lengths, therefore, intersects the boundaries at right angles.

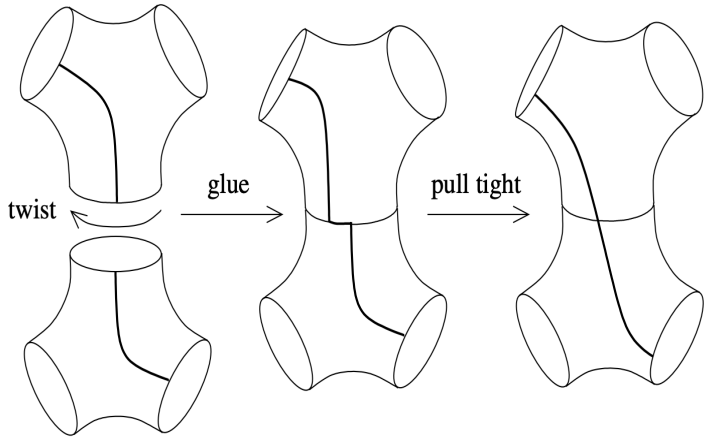

Figure 18. A visualization of what the twisting angle represents and measures. By twisting the orientation of the pants before gluing them, we end up with a different isometry type.

Definition 5.5. For two pants P_1 and P_2 that are glued together along γ_i, the shortest path τ_1 on P_1 intersects γ_i at p_1, and the shortest path τ_2 on P_2 intersects γ_i at p_2. The **twisting angle** - sometimes also referred to as the twisting parameter - is given by:

$$\theta = 2\pi \frac{d(p_1, p_2)}{|\gamma|}$$

where $d(p_1, p_2)$ is the geodesic distance between p_1 and p_2 and $|\gamma|$ is the length of γ.

To visualize twisting angles, let's suppose we're gluing two pairs of pants to create a surface S. If we simply glued the pants in the orientation shown in the leftmost image of figure 18, it would be different to gluing pants as shown in the rightmost image. This is because the geodesic distance $d(p_1, p_2)$ is different, which would change the twisting angle. Therefore, rotating the top pair of pants changes the pants composition, which is why keeping track of the twisting angle is important.

Definition 5.6. For a surface S of $g > 1$, S can be decomposed in $2g - 2$ pairs of pants $\{P_1, P_2, ...P_{2g-2}\}$ by closed geodesics $\{\gamma_1, \gamma_2, ..., \gamma_{3g-3}\}$. The **Fenchel-Nielson coordinates** of S in a Teichmüller space $T_{g,n}$ are given by:

$$\{(|\gamma_1|, \theta_1), (|\gamma_2|, \theta_2), ..., (|\gamma_{3g-3}|, \theta_{3g-3})\}.$$

We can now prove our main theorem.

Theorem 5.7. *Let $g \geq 2$ for a surface S. The map*

$$FN : T_S \to \mathbb{R}_+^{3g-3} \times \mathbb{R}^{3g-3}$$

defined by

$$FN(X) = (|\gamma_1|, |\gamma_2|, ..., |\gamma_{3g-3}|, \theta_1, \theta_2, ..., \theta_{3g-3})$$

is a homeomorphism.

Proof. Another way to interpret this theorem is $T_g \approx \mathbb{R}^{6g-6} \cong \mathbb{C}^{3g-3}$.

First, realize that the theorem is essentially saying that a point on the Teichmüller space determined by the Fenchel-Nielson coordinates can also be expressed by $\mathbb{R}_+^{3g-3} \times \mathbb{R}^{3g-3}$. One way to approach this is to construct our pants decomposition and essentially "count" the inputs that determine this point - sort of like a probability problem. There are two parts that we have to consider. To tackle this construction, first we consider how we glue the pants together. Then, we consider the orientation of the pants when we're gluing.

Let's start with how we glue the pants together. Recall that proposition 5.3 states that a triple of positive real numbers can define the alternating edges of a hyperbolic right-angled hexagon. This means that choosing three real values determines the hexagon that makes up a pair of pants. Since this is the seam - as defined in definition 5.2 - and the seam essentially defines the shape of the pants, the three real values that we choose determine what the pants look like and the geodesics on it that can be glued to other geodesics on other pants. Additionally, by proposition 5.4, we know that there are $2g - 2$ pairs of pants. So in total, we have $3(2g - 2) = 6g - 6$ curves. However, note that we count these curves in pairs, which means we end up with $\frac{6g-6}{2} = 3g - 3$ total curves in a pants decomposition. Thus, $3g - 3$ lengths (which are positive real values) determine the ways in which what sized pants are glued together.

Next, we tackle the orientation of the pants when we're gluing them together. Recall the twisting angle as defined in definition 5.5. The twisting angles are defined from 1 to $3g - 3$.

Note that even if we twist the pants by a 2π revolution, the orientation is still different. This is because revolving by 2π results in a different length for the geodesic. Doing a $n\pi$ revolution - even if n is even - ends up with a different composition.

Therefore, $\mathbb{R}_+^{3g-3}$ represents "choosing" the lengths of the hexagon, and $\mathbb{R}^{3g-3}$ represents the twist between pants. Thus, $\mathbb{R}_+^{3g-3} \times \mathbb{R}^{3g-3}$ represents a point on the Teichmüller space T_g. The Fenchel-Nielson coordinates also represent points on Teichmüller spaces. This concludes the proof. ■

To perform this proof more rigorously, more work is required though it is slightly uninteresting. See [FM11] for the more rigorous proof.

6. Further Research Regarding Teichmüller Spaces

The study of Teichmüller spaces is called Teichmüller theory. This field is being actively studied, and there are several interesting theorems that arise from Teichmüller spaces. For example, in [referece], M_g is defined as the moduli space of Riemann surfaces, and $N(R)$ is defined as the number of closed Teichmüller geodesics in M_g of length at most R.

Theorem 6.1. *As $R \to \infty$, we have*

$$N(R) \sim \frac{e^{hR}}{hR}$$

where $h = 6g - 6$

The notation $A \sim B$ means the ratio $\frac{A}{B}$ tends to 1. Another theorem - conveniently named Teichmüller's theoem - states:

Theorem 6.2. *For two marked Riemann surfaces (X, g) and (Y, h), there's always a unique quasiconformal mapping $X \to Y$ in the isotopy class of $h \circ g^{-1}$ which has a minimal dilation. This map is called the Teichmüller mapping.*

Furthermore, there are several metrics that arise to study the metric geometry of Teichmuüller space. For example, the Teichmüller metric is:

Definition 6.3. If $x, y \in T_S$ and the Teichmüller mapping between them has dilatation K then the Teichmüller distance between them is by definition $\frac{1}{2}\log(K)$.

This metric defines a distance on T_S that induces its topology. There's also the Weil-Petersson metric that's commonly paired with Fenchel-Nielson Coordinates to study Teichmüller spaces. See [Wei58] for more detail on them.

In general, as mentioned earlier, Teichmüller spaces provide a lot of insight into moduli spaces and allow us to study moduli spaces more in-depth. Furthermore, Teichmüller spaces can be used for real-world applications, particularly in scientific research.

References

[Bro18] Jennifer Brown. Teichmüller spaces. 2018.

[FM11] Benson Farb and Dan Margalit. *A primer on mapping class groups (pms-49)*. Princeton university press, 2011.

[FN03] Werner Fenchel and Jakob Nielsen. *Discontinuous groups of isometries in the hyperbolic plane*, volume 29. Walter de Gruyter, 2003.

[JZDG09] Miao Jin, Wei Zeng, Ning Ding, and Xianfeng Gu. Computing fenchel-nielsen coordinates in teichmuller shape space. In *2009 IEEE International Conference on Shape Modeling and Applications*, pages 193–200. IEEE, 2009.

[SZS+16] Rui Shi, Wei Zeng, Zhengyu Su, Jian Jiang, Hanna Damasio, Zhonglin Lu, Yalin Wang, Shing-Tung Yau, and Xianfeng Gu. Hyperbolic harmonic mapping for surface registration. *IEEE transactions on pattern analysis and machine intelligence*, 39(5):965–980, 2016.

[Tel03] C Teleman. Riemann surfaces. *Online Lecture Notes: http://math. berkeley. edu/teleman/math/Riemann. pdf*, 2003.

[Wei58] André Weil. On the moduli of riemann surfaces. *Oeuvres Scient*, 2:381–389, 1958.